Electronic Supporting Information

Mechanistic studies on the addition of hydrogen to iridaepoxide complexes with subsequent elimination of water.

Lauren E. Doyle, Warren E. Piers,* Javier Borau-Garcia, Michael J. Sgro, Denis M. Spasyuk

University of Calgary, Department of Chemistry, 2500 University Drive N.W., Calgary, Alberta, Canada, T2N 1N4.

Contents

General Considerations. Storage and manipulation of all compounds were performed under an argon atmosphere either in a VAC glove box or using a double manifold high vacuum line using standard techniques. Toluene, pentane and hexanes were dried and purified using a Grubbs/Dow solvent purification system and stored in 500 mL thick-walled vessels over sodium/benzophenone ketal. Dichloromethane and dichloromethane-d_2 were dried over calcium hydride and vacuum transferred into thick-walled vessels for storage over activated sieves. Toluene-d_8 was dried and stored over sodium/benzophenone ketal. All dried solvents were degassed and vacuum distilled prior to use. ^{1}H and ^{13}C NMR chemical shifts were referenced to residual solvent protons and naturally abundant ^{13}C resonances for all deuterated solvents. Chemical shift assignments are based on ^{1}H, $^{13}C\{^{1}H\}$, $^{31}P\{^{1}H\}$, ^{19}F, ^{1}H-^{1}H-COSY, ^{1}H-^{13}C-HSQC and ^{1}H-^{13}C-HMBC NMR experiments performed on Bruker RDQ-400, Ascend-500 or Avance-600 spectrometers. Deuterium (99.7%) and Ultra High Purity Hydrogen were purchased from Praxair and used as received. Nitrous oxide (99%) and deuterium hydride (96 mol%, 98 atom % D) were purchased from Sigma-Aldrich and used as received. All other reagents were purchased from Sigma-Aldrich and used as received. X-ray crystallographic analyses were performed on either a Nonius KappaCCD diffractometer or a Bruker Smart diffractometer equipped with Apex II detector. Samples were coated in Paratone 8277 oil (Exxon) and mounted on a glass fibre. Full crystallography details can be found in independently uploaded .cif files. All Elemental analyses were obtained by the Instrumentation Facility of the Department of Chemistry, University of Calgary.

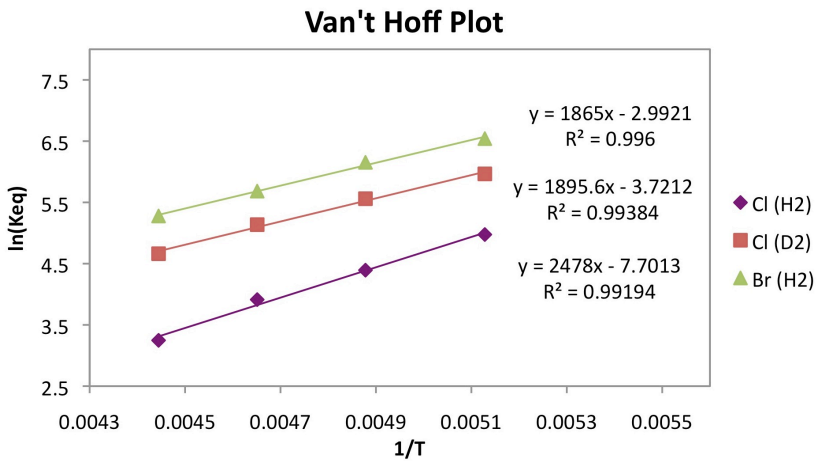

$$K_{eq} = \frac{[2\bullet X_{cis}]}{[1\bullet X][H_2]}$$

T (°C)	$[H_2]$ (mM)
-78	3.07
-68	3.27
-58	3.47
-48	3.67

Figure S1. *Left*: Van't Hoff plots depicting the equilibrium of **1•Cl** and **2•Cl$_{cis}$** with H_2 (purple diamonds), **1•Cl** and **2•Cl$_{cis}$** with D_2 (red squares) and **1•Br** and **2•Br$_{cis}$** with H_2 (green triangles). *Right*: Equation for the equilibrium constant and concentrations of H_2 (mM) in CD_2Cl_2 at varying temperatures measured by ^{1}H NMR spectroscopy.

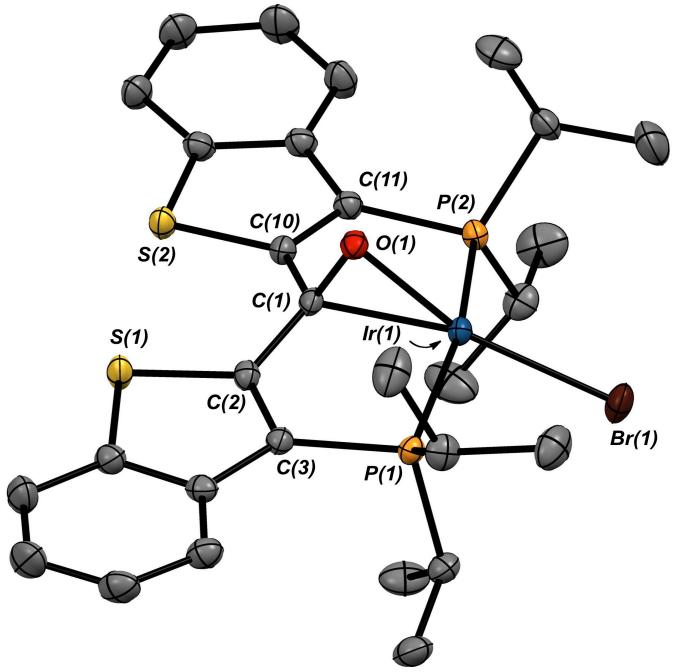

Figure S2. Molecular structure of **1•Br**. Hydrogen atoms have been omitted for clarity. Displacement ellipsoids are shown at the 50% probability level. Selected bond lengths (Å): Ir(1)-P(1), 2.3214(6); Ir(1)-P(2), 2.3234(6); Ir(1)-C(1), 2.4387(3); Ir(1)-O(1), 2.0489(17); Ir(1)-Br(1), 2.4387(3); C(1)-O(1), 1.355(3). Selected bond angles (˚): C(1)-Ir(1)-O(1), 38.23(8); C(1)-O(1)-Ir(1), 72.42(12); Ir(1)-C(1)-O(1), 69.36(12); P(1)-Ir(1)-P(2), 162.57(2).

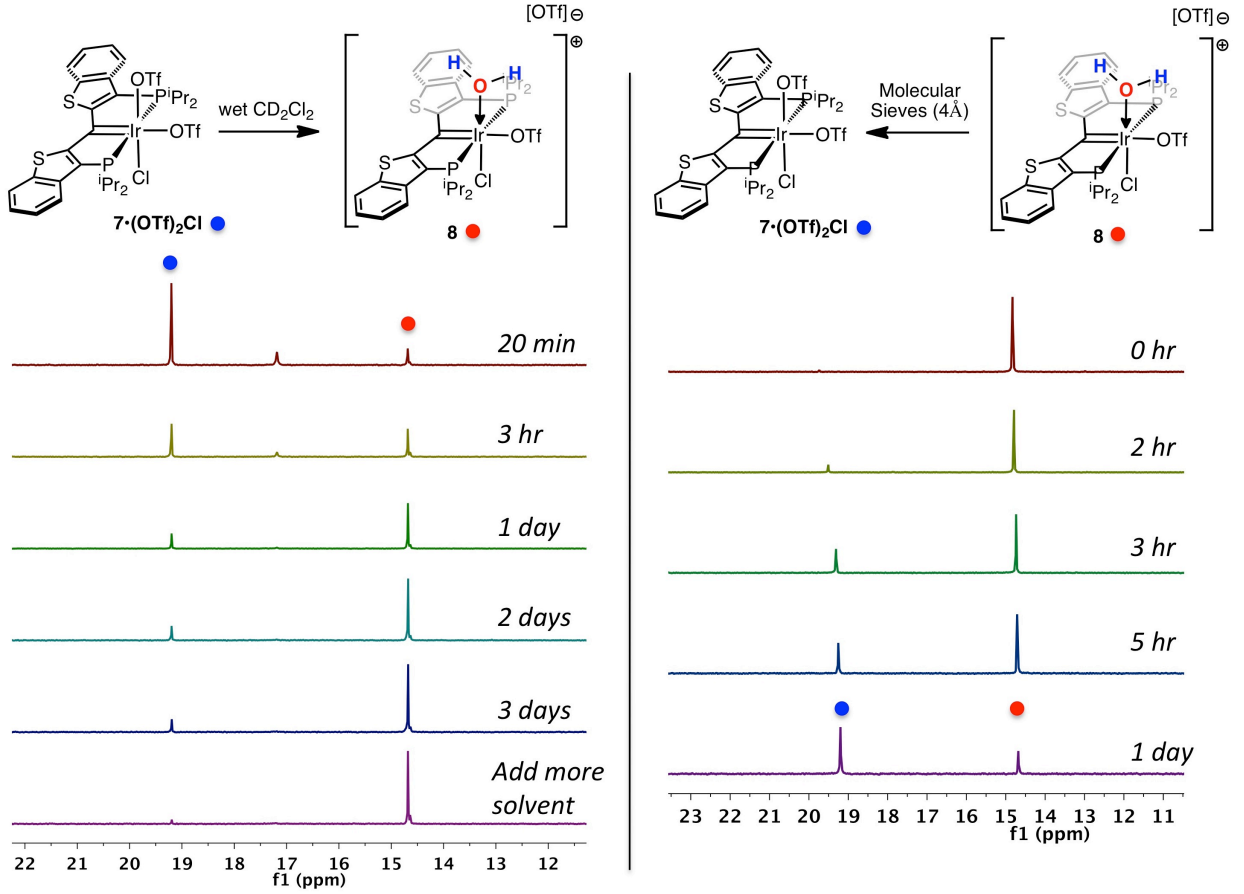

Figure S3. *Left*: $^{31}P\{^{1}H\}$ NMR spectra (CD_2Cl_2, 203 MHz, 25 °C) of **7•(OTf)$_2$Cl** dissolved in wet CD_2Cl_2 over time. The bottom spectrum was taken after more CD_2Cl_2 (wet) was added to the sample. *Right*: $^{31}P\{^{1}H\}$ NMR spectra (CD_2Cl_2, 203 MHz, 25 °C) over time of a solution of **8** mixed with a few activated molecular sieves (4Å).

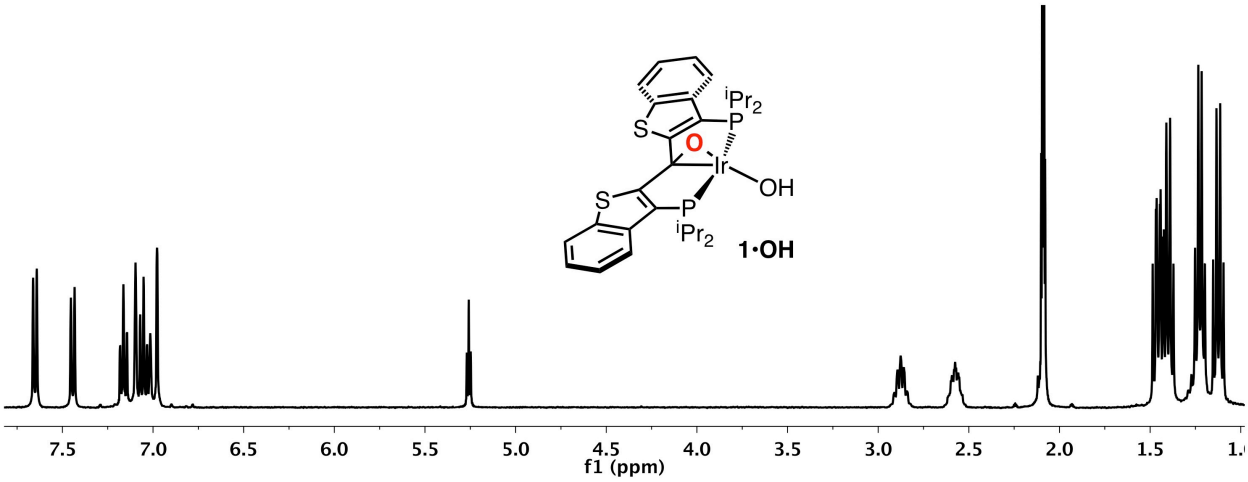

Figure S4. ^{1}H NMR spectrum of **1•OH** in toluene-d_8.

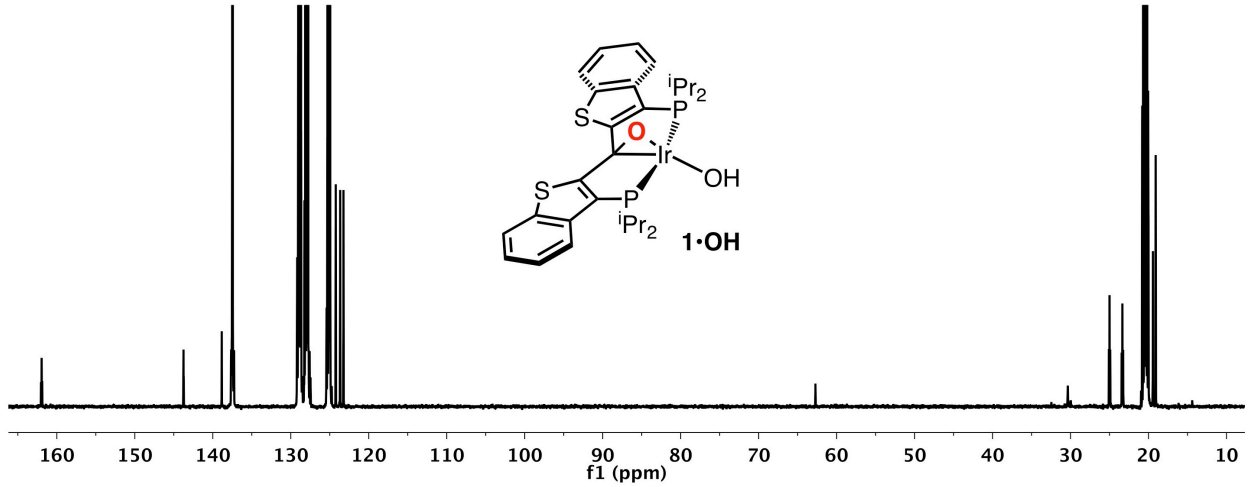

Figure S5. $^{13}C\{^{1}H\}$ NMR spectrum of **1•OH** in toluene-d_8.

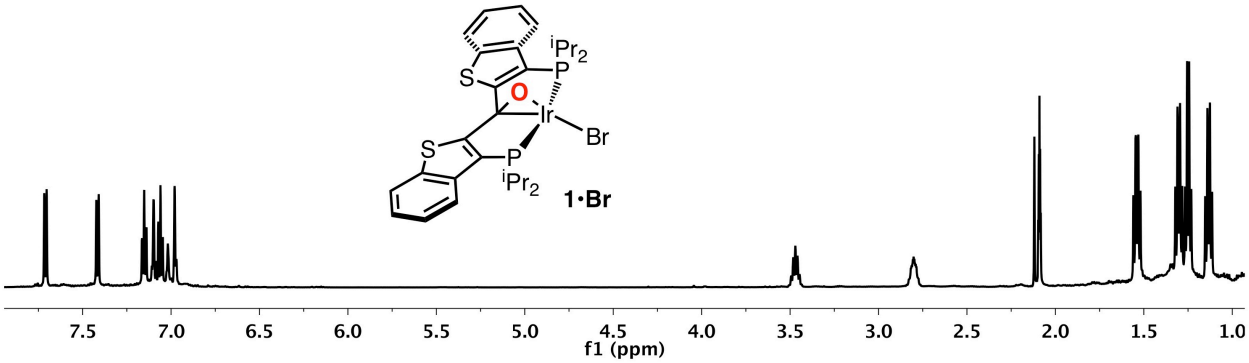

Figure S6. ^{1}H NMR spectrum of **1•Br** in toluene-d_8.

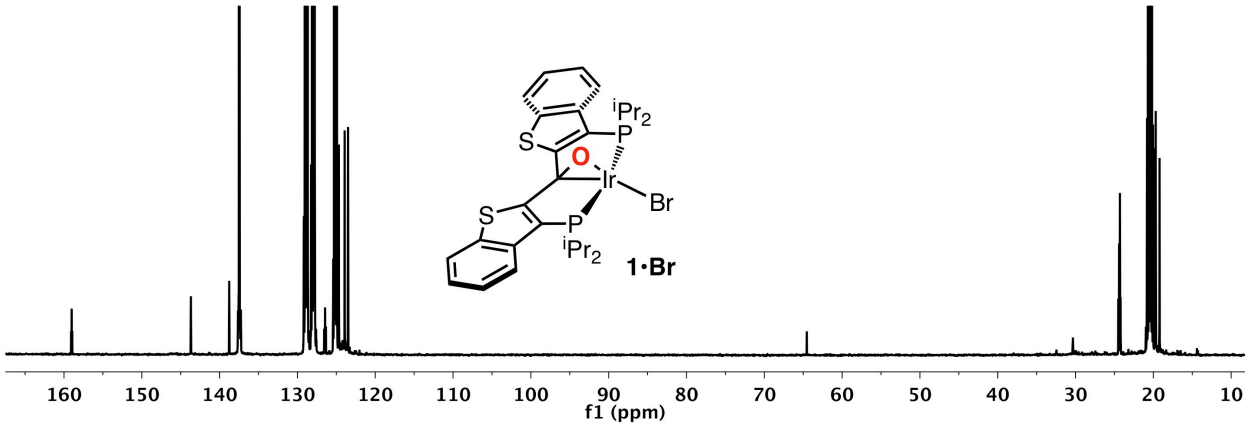

Figure S7. $^{13}C\{^{1}H\}$ NMR spectrum of **1•Br** in toluene-d_8.

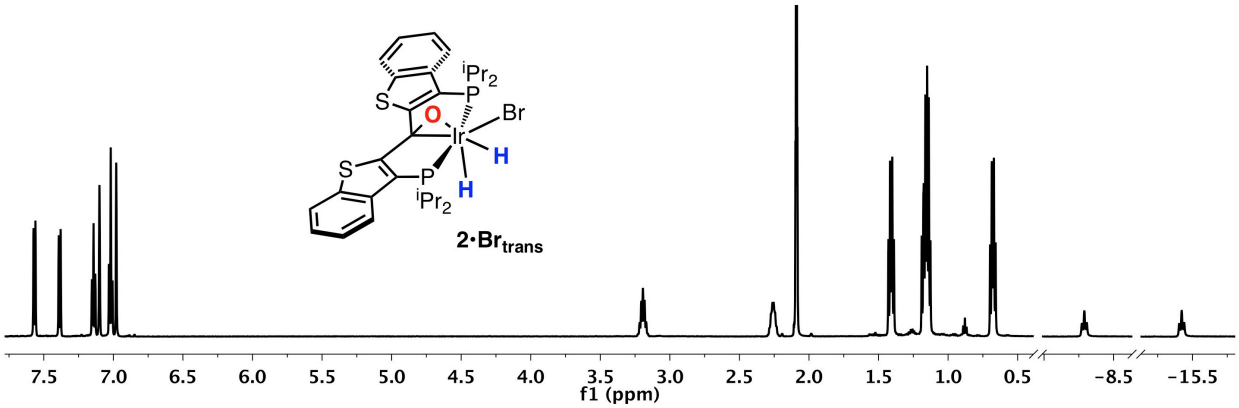

Figure S8. ^{1}H NMR spectrum of **2•Br$_{trans}$** in toluene-d_8.

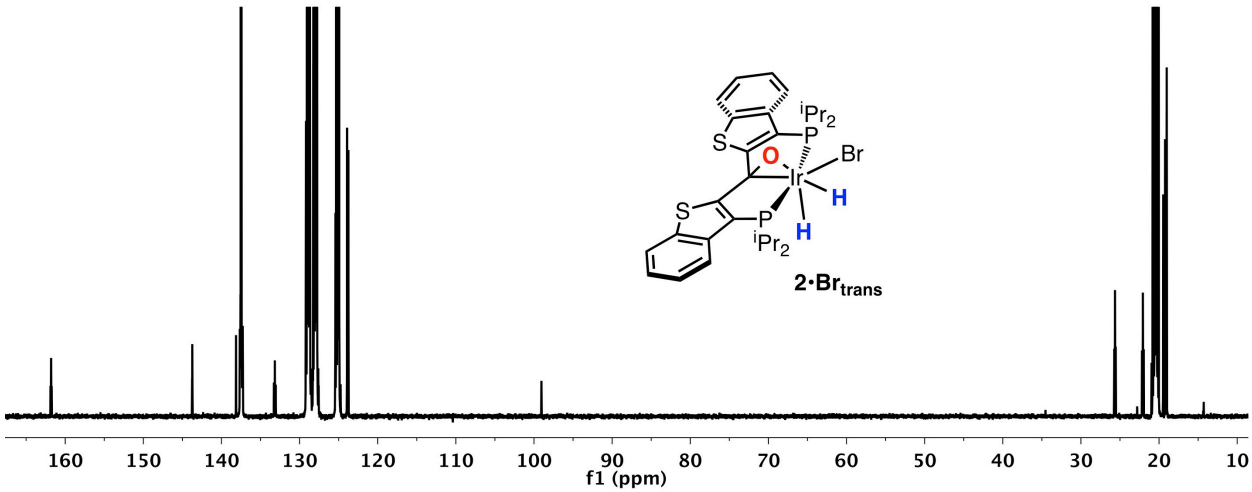

Figure S9. ^{13}C{^{1}H} NMR spectrum of **2•Br$_{trans}$** in toluene-d_8.

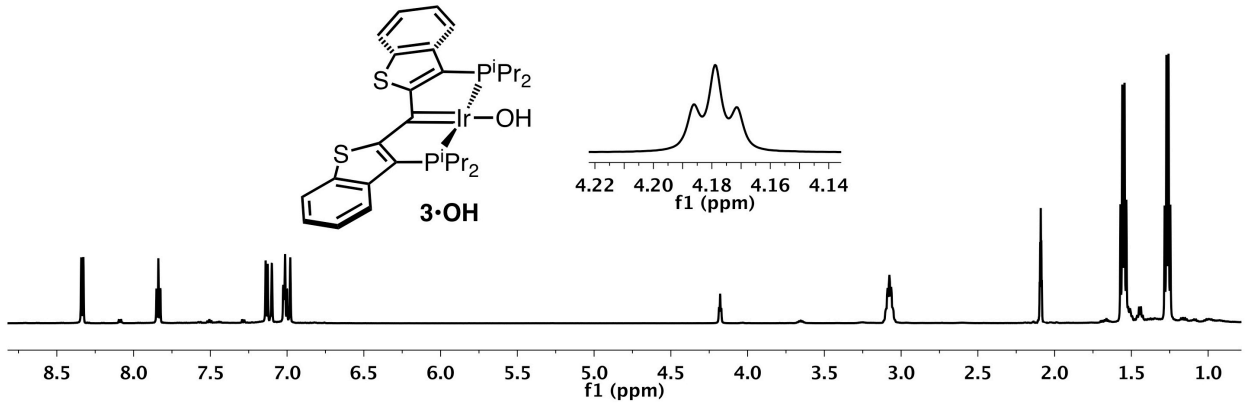

Figure S10. ^{1}H NMR spectrum of **3•OH** in toluene-d_8.

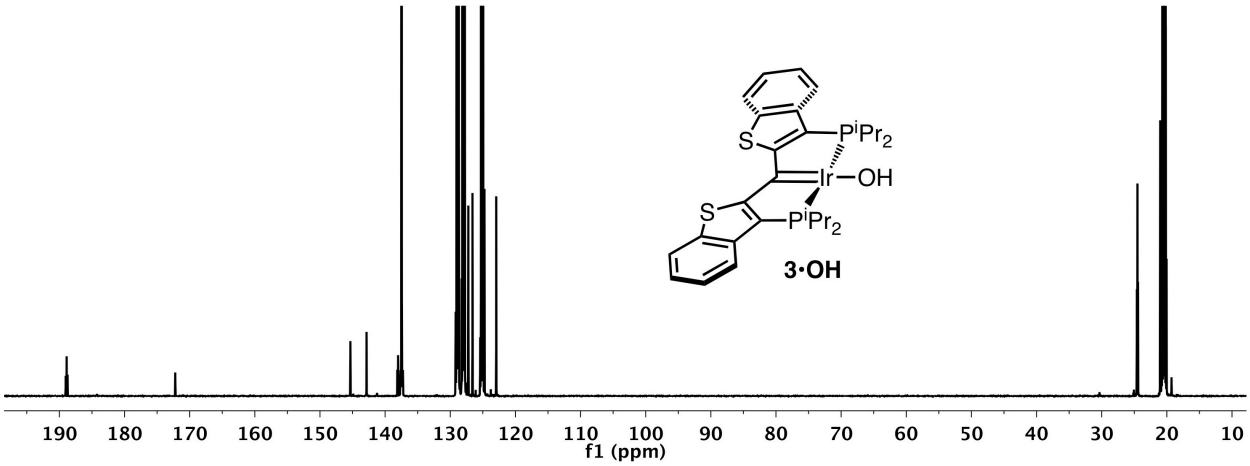

Figure S11. $^{13}C\{^{1}H\}$ NMR spectrum of **3•OH** in toluene-d_8.

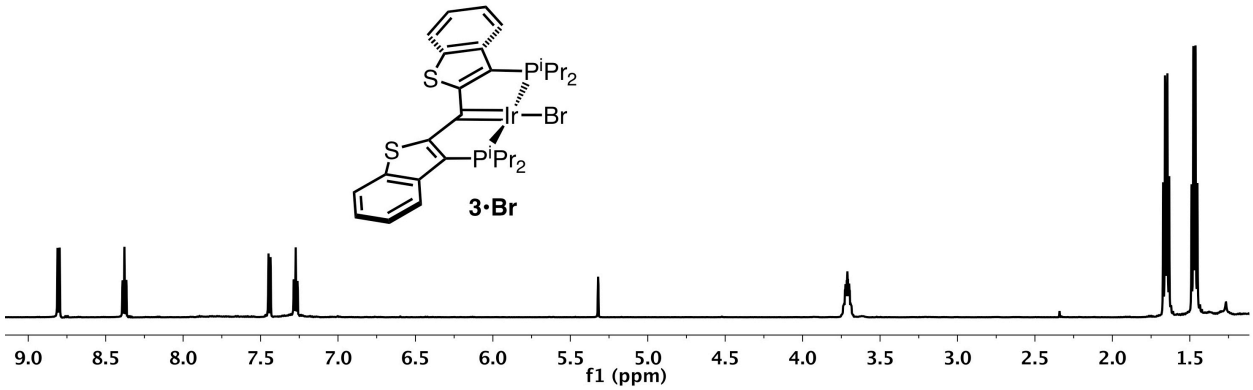

Figure S12. ^{1}H NMR spectrum of **3•Br** in CD_2Cl_2.

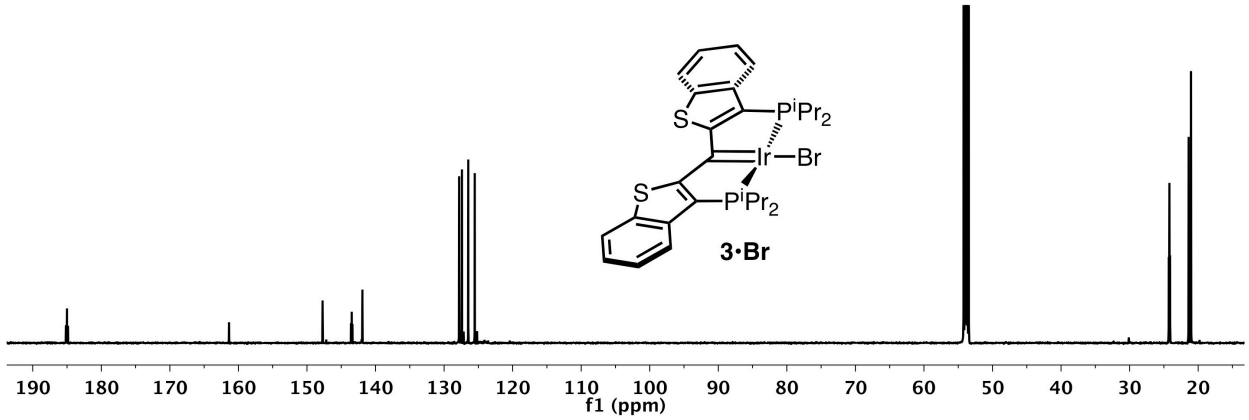

Figure S13. $^{13}C\{^{1}H\}$ NMR spectrum of **3•Br** in CD_2Cl_2.

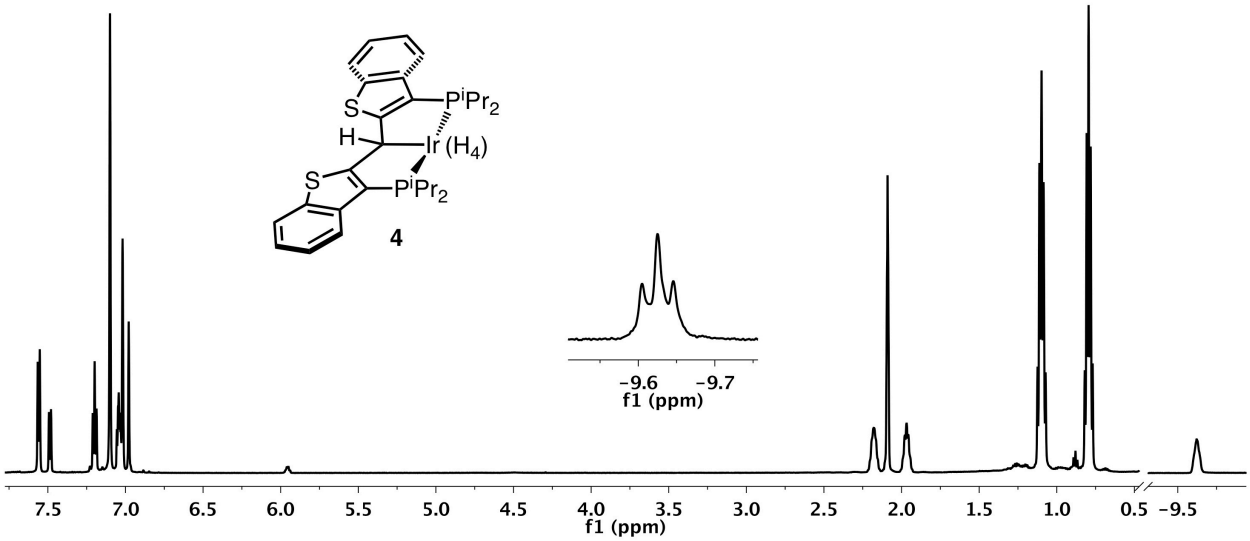

Figure S14. ^{1}H NMR spectrum of **4** in toluene-d_8. The inset shows a triplet at -9.63 ppm before full conversion to **4** and before substantial H/D exchange had occurred.

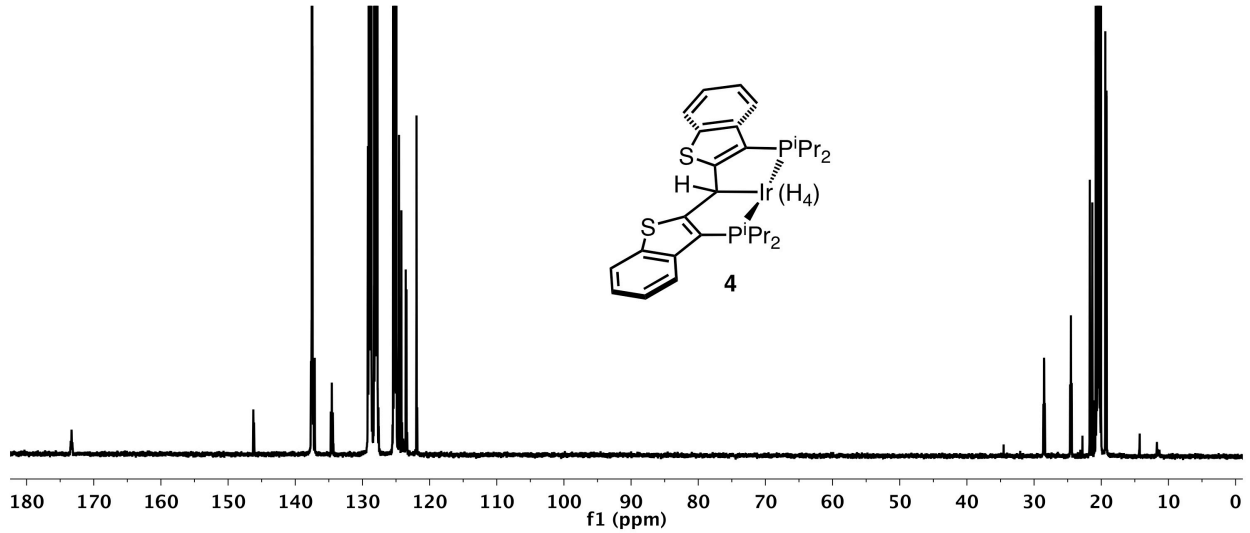

Figure S15. ^{13}C{^{1}H} NMR spectrum of **4** in toluene-d_8.

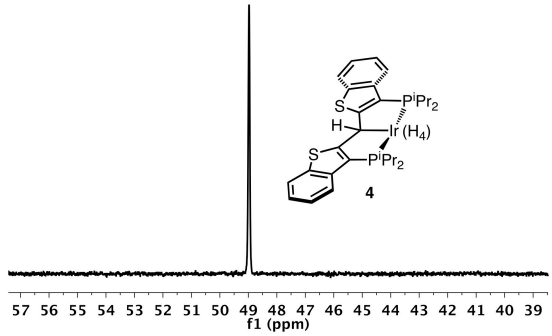

Figure S16. ^{31}P{^{1}H} NMR spectrum of **4** in toluene-d_8.

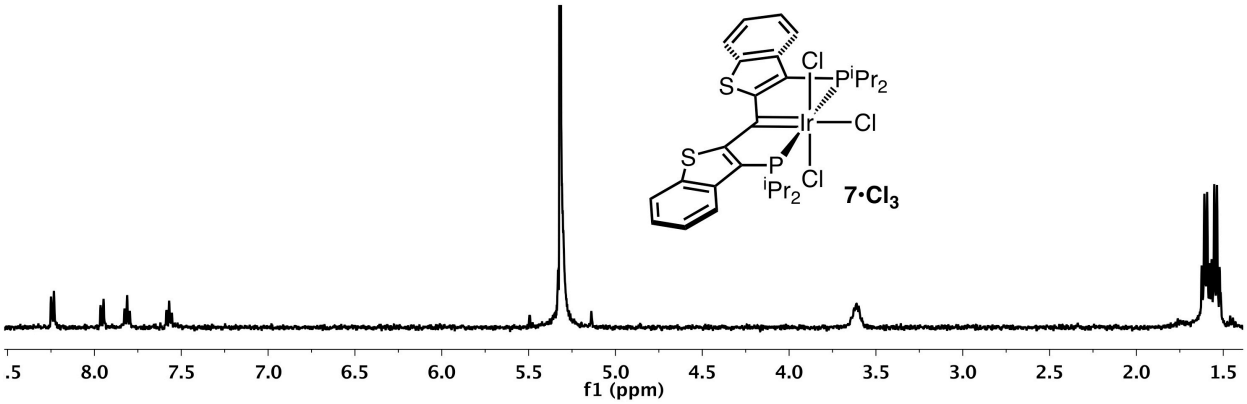

Figure S17. ^{1}H NMR spectrum of **7•Cl$_3$** in CD_2Cl_2.

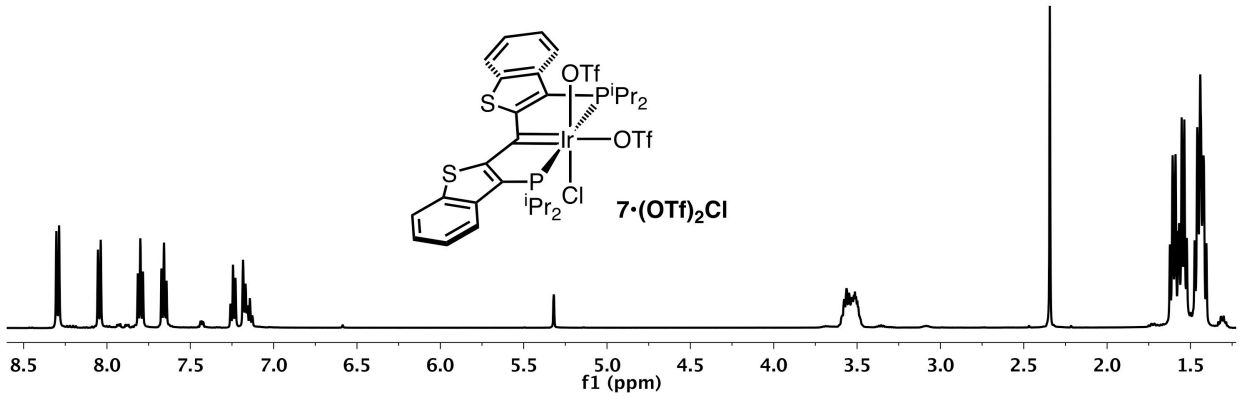

Figure S18. ^{1}H NMR spectrum of **7•(OTf)$_2$Cl** in CD_2Cl_2.

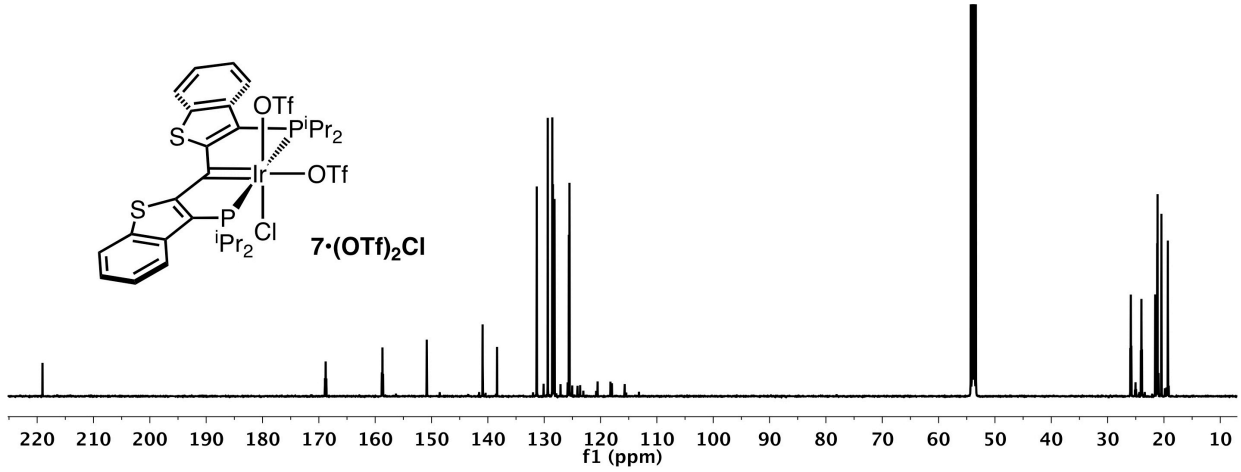

Figure S19. ^{13}C{^{1}H} NMR spectrum of **7•(OTf)$_2$Cl** in CD_2Cl_2.

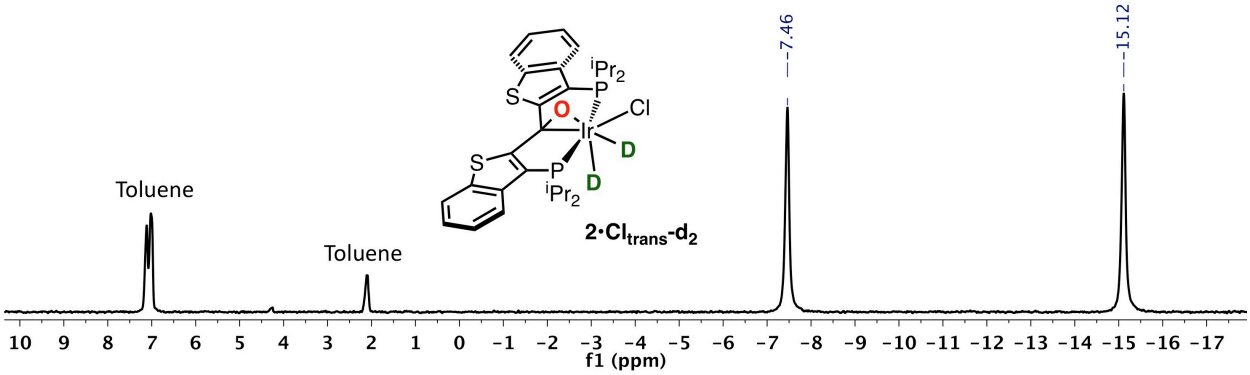

Figure S20. ^{2}H NMR spectrum of **2•Cl$_{trans}$-d$_2$** in toluene.

Table S1. Data collection and structure refinement details for **3•OH**, **1•OH**, **1•Br**, **7•Cl_3**, **7•$(OTf)_2Cl$**, and **8**.

	3•OH	**1•OH**	**1•Br**	**7•Cl_3**	**7•$(OTf)_2Cl$**	**8**
formula	$C_{29}H_{37}IrOP_2S_2$	$2(C_{29}H_{36}IrO_2P_2S_2)$, C_7H_8	$C_{29}H_{36}BrIrOP_2S_2$, C_7H_8	$C_{29}H_{36}Cl_3IrP_2S_2$, C_7H_8	$C_{31}H_{36}ClF_6IrO_6P_2S_4$	$C_{30}H_{38}ClF_3IrO_4P_2S_3$, CO_3SF_3
fw	719.84	1561.81	890.88	901.32	1036.43	1054.44
crystal system	monoclinic	triclinic	monoclinic	monoclinic	monoclinic	monoclinic
space group	P21/c	P-1	P21/n	P21/c	C2/c	C2/c
a, Å	13.5212(3)	12.8155(7)	14.5417(3)	12.4862(3)	29.3975(5)	27.4764(5)
b, Å	15.0131(4)	14.1374(8)	11.2071(2)	13.6671(5)	17.9182(3)	20.4688(4)
c, Å	16.0250(2)	19.4358(11)	22.7055(5)	23.6020(6)	23.5916(6)	18.4422(4)
α, deg	90	105.409(2)	90	90	90	90
β, deg	116.7160(10)	103.594(2)	106.9590(10)	118.383(2)	122.6490(10)	112.8740(10)
γ, deg	90	93.729(2)	90	90	90	90
V, Å^3	2905.73(11)	3269.0(3)	3539.41(13)	3543.51(19)	10463.3(4)	9556.4(3)
Z	4	2	4	4	8	8
T, K	173(2)	173(2)	173(2)	173(2)	173(2)	173(2)
λ, Å	0.71073	1.54178	1.54178	0.71073	1.54178	1.54178
ρ_{calc}, g/cm^3	1.645	1.587	1.672	1.689	1.316	1.466
F(000)	1432	1560	1768	1800	4096	4176
μ, mm^{-1}	4.869	10.236	10.789	4.229	7.944	8.724
crystal size, mm^3	0.08×0.06×0.04	0.25×0.150×0.110	0.20×0.20×0.20	0.04×0.04×0.02	0.15×0.1×0.1	0.18×0.09×0.09
transmission factors	0.6967 – 0.8291	0.552 – 0.753	0.3974 – 0.5230	0.8491 – 0.9202	0.3820 – 0.5038	0.4746 – 0.7531
θ range, deg	1.966 – 24.999	2.444 – 67.493	3.235 – 67.490	2.379 – 24.998	3.045 – 66.500	3.308 – 68.419
data/restraints/param	5061/2/320	11415/729/730	6367/387/397	6180/570/425	9117/0/468	8633/150/525
GoF	1.044	1.031	1.073	1.132	1.018	1.037
R_1 ($I>2\sigma(I)$)	0.0276	0.0356	0.0201	0.0552	0.0497	0.0391
wR_2 (all data)	0.0682	0.0917	0.0497	0.1511	0.1441	0.1089
residual density, e/Å^3	1.216 and -0.659	2.780 and -1.149	0.439 and -0.849	1.332 and -0.798	2.243 and -0.732	0.982 and -0.870